

# Adaptive Hybrid Visual Servoing/Force Control in Unknown Environment

Koh Hosoda, Katsuji Igarashi, and Minoru Asada

Department of Mech. Eng. for Computer-Controlled Machinery  
 Faculty of Engineering, Osaka University  
 Suita, Osaka 565, Japan

## Abstract

*This paper describes an adaptive hybrid visual servoing/force controller to realize visual servoing while the manipulator exerts contact force on a surface. The proposed controller has a hybrid structure of visual servoing control and force control. Because it has an on-line estimator for the parameters of the camera-manipulator system and the one for the parameters of the unknown constraint surface, it only needs a priori knowledge on the manipulator kinematics and nothing any more.*

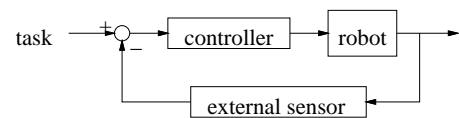
*First, we propose an estimator for an image Jacobian matrix which describes the relation between image features and the tip position/orientation of the manipulator. Second, a method to estimate the normal vector of the unknown constraint surface is introduced. Then, an adaptive hybrid visual servoing/force controller is proposed. Finally, experimental results are shown to demonstrate the effectiveness of the proposed scheme.*

## 1 Introduction

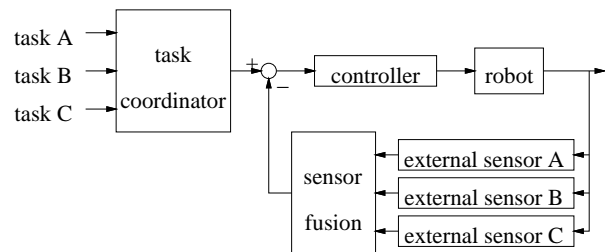
External sensors, such as cameras, range finders, force sensors et al., play a great role for a robot to accomplish given tasks in unknown/dynamic environments. By utilizing these external sensors, the robot can observe states of the robot, states of the environment, and task performance of the robot from various kinds of viewpoints of different sensor modalities. Further, the robot might be calibration free, fault tolerant, and disturbance free. In order to cope with the higher requirements of the robot task performance, combination of these external sensors seems indispensable.

A task given for such a robot equipped with several external sensors is decomposed into subtasks which are independently defined in the corresponding external sensor spaces, and should be accomplished at the same time. In such a case, one have to coordinate several external sensor based controllers, and the resultant controller becomes a *hybrid structure* of several external sensor based controllers (figure 1 (C)).

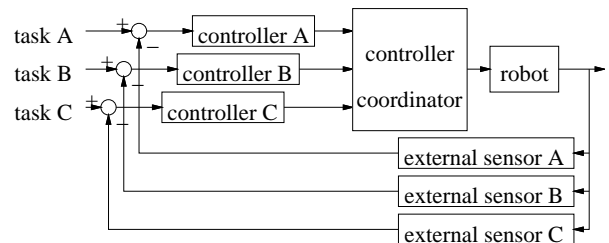
There have been many studies on only one external sensor case (figure 1 (A)), for example, on the vision sensor [1–7], or on the force sensor [8–10]. In these cases, however, the task definition is limited with one



(A) single external sensor based control



(B) multi external sensor based control with sensor-fusion



(C) hybrid structure of external sensor based control

Figure 1: structure of various controllers

sensor's capability, and therefore the task which the robot can do is limited.

If the robot has multi sensors, it is common to use the fusion of the sensing results, so-called sensor-fusion (figure 1(B)). However, in order to build a fast and robust robot, it is more important to coordinate the external sensor based controllers than to coordinate the sensory data in the perception stage, because a fusion process often needs time-consuming procedures.

Nelson et al. has proposed multi sensor based hybrid visual servoing/force control in [11]. In their approach, the tasks are well-considered beforehand so that the tasks can be independent of each other. But, such a controller suffers from disturbance and tasks

on the sensor spaces must be given independently in general. Therefore, it is needed to develop a method to coordinate external sensor based controllers. To the best of our knowledge, there has been no research on such a hybrid structure of external sensor based controllers.

In this paper, focusing on hybrid structure of several external sensor based controllers, an adaptive hybrid visual servoing/force controller is proposed. The proposed controller has hybrid structure consisting of force control and visual servoing control. The task given for the robot also consists of a force exerting task and a visual servoing task, and they are not coordinated beforehand. The visual servoing controller has an on-line estimator for the parameters of the camera-manipulator system, which is already proposed and validated by the authors' group[12]. The force controller also has an on-line estimator for the parameters of the unknown constraint surface, therefore, the proposed controller only needs knowledge on the manipulator kinematics and nothing anymore. However, these controllers estimate their own parameters independently, one have to coordinate the estimated results on-line.

The remainder of this article is organized as follows. First, we propose an estimator for the image Jacobian matrix which describes the relation between image features and the tip position/orientation of the manipulator. Second, a method to estimate the normal vector of an unknown constraint surface is introduced. Then, an adaptive hybrid visual servoing/force controller is proposed. Finally experimental results are shown to demonstrate the effectiveness of the proposed estimators and controller.

## 2 Task and assumptions for the camera-manipulator system

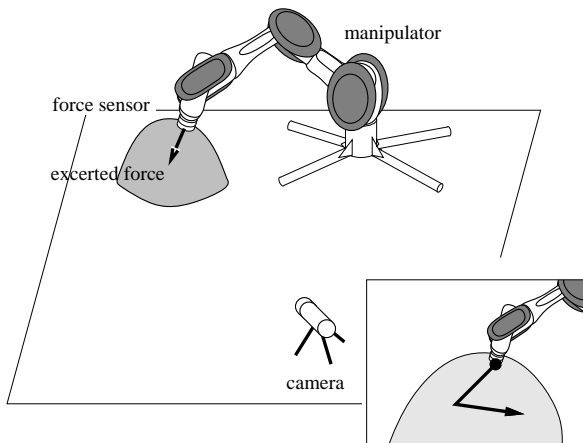


Figure 2: Camera-manipulator system

A camera-manipulator system consisting of a manipulator and a camera is shown in figure 2. Utilizing the camera, one can observe quantities of image

features such as position, line length, contour length, and/or area of certain image regions. The image features are on the tip of the manipulator. The manipulator has a force sensor at the tip.

The task of the camera-manipulator system is to make the quantities of image features converge to given desired trajectories while the force at the tip of the manipulator also converge to the desired one. Here, we assume that

**A1** the only knowledge that the controller has is the kinematics of the manipulator, position/orientation of the manipulator tip with respect to the manipulator base frame, and nothing any more. That is, it does not have any *a priori* knowledge on the translation/rotation between the manipulator base frame and the camera frame, on the camera model, on the constraint surface, nor on the relation between the manipulator and the constraint surface, and that

**A2** the number of constraint surface is one, but its equation is unknown. This means that the end-effector position is constrained on an unknown smooth 2-D curved surface. The constraint surface is assumed in  $C_1$  class.

## 3 Estimation of image Jacobian matrix

Let  $\mathbf{x} \in \mathbb{R}^n$  and  $\mathbf{x}_{img} \in \mathbb{R}^m$  denote the position/orientation vector with respect to the manipulator base frame and the image feature vector obtained from the camera, respectively. Let the relation between  $\mathbf{x}$  and  $\mathbf{x}_{img}$  be

$$\mathbf{x}_{img} = \mathbf{x}_{img}(\mathbf{x}). \quad (1)$$

Differentiating eq.(1), we get a velocity relation,

$$\dot{\mathbf{x}}_{img} = \mathbf{E}_{img}(\mathbf{x})\dot{\mathbf{x}}, \quad (2)$$

where  $\mathbf{E}_{img}(\mathbf{x}) = \partial \mathbf{x}_{img} / \partial \mathbf{x}^T \in \mathbb{R}^{m \times n}$  is so called an image Jacobian matrix that describes the relation between time-derivatives of the quantities of image features with respect to the position/orientation of the tip of the manipulator. This Jacobian matrix is dependent on the internal camera parameters such as focal length, aspect ratio, distortion coefficients, and the relative position and orientation of the camera with respect to the manipulator base frame.

Assuming that movement of the camera-manipulator system is slow enough to consider the image Jacobian matrix  $\mathbf{E}_{img}$  as constant during the sampling time, we get

$$\mathbf{x}_{img}(k+1) = \mathbf{x}_{img}(k) + \mathbf{E}_{img}(k)\mathbf{u}(k), \quad (3)$$

as a discrete model of the image features, where  $\mathbf{E}_{img}(k)$  and  $\mathbf{u}(k)(= T\dot{\mathbf{x}})$  denote the constant Jacobian matrix and a control input vector in  $k$ -th step during sampling rate  $T$ , respectively.

So as to estimate  $i$ -th row vector of the matrix  $\mathbf{E}_{img}$ ,  $\mathbf{e}_i^T$ , which satisfies eq.(3), we utilize a kind

of least squares method to identify non-linear systems in discrete time domain [13]:

$$\begin{aligned} & \hat{\mathbf{e}}_i(k+1) - \hat{\mathbf{e}}_i(k) \\ &= \frac{\{\mathbf{x}_{img}(k+1) - \mathbf{x}_{img}(k) - \hat{\mathbf{E}}_{img}(k)\mathbf{u}(k)\}_i}{\rho_i + \mathbf{u}(k)^T \mathbf{W}_i(k) \mathbf{u}(k)} \cdot \\ & \quad \mathbf{W}_i(k) \mathbf{u}(k), \quad (4) \end{aligned}$$

where  $\mathbf{W}_i(k)$  and  $\rho_i$  denote a weighting matrix and an appropriate positive constant that ensures stability of eq.(4), respectively. When  $\|\mathbf{u}\|$  tends to 0, the denominator tends to  $\rho_i$  and the stability is ensured even if the numerator does not tend to 0 because of disturbances. The positive constant  $\rho_i$  is determined so small that  $\rho_i$  can be neglected with respect to  $\|\mathbf{u}\|$  when  $\|\mathbf{u}\|$  is large.

The proposed estimator is intended not to estimate the true Jacobian matrix, but to estimate a matrix that satisfies eq.(3). By utilizing the estimated image Jacobian matrix, the authors have already shown that we can apply visual servoing control to uncalibrated camera-manipulator systems [12].

#### 4 Estimation of unknown constraint surface[9]

According to the assumption **A2**, the constraint surface is represented as

$$S(\mathbf{x}) = 0. \quad (5)$$

Differentiating eq.(5), we get

$$\mathbf{e}_f^T \dot{\mathbf{x}} = 0. \quad (6)$$

Because the controller does not have any *a priori* knowledge on the constraint surface (assumption **A1**), the normal vector of the surface  $\mathbf{e}_f$  has to be estimated from the signals of sensors.

Suppose that the tip of the manipulator keeps contact with the surface, and we can observe force  $\mathbf{f}$  from the force sensor as the sum of the frictional force and the normal force (figure 3). By assuming that the frictional force is in the direction of end-effector motion, we can calculate the estimated unit normal vector  $\hat{\mathbf{e}}_f$ . Let  $\Delta\mathbf{x}$  be the end effector motion during sampling rate  $T$ , and the estimated vector  $\tilde{\mathbf{e}}_f$  becomes

$$\tilde{\mathbf{e}}_f = \tilde{\mathbf{f}} / \|\tilde{\mathbf{f}}\|, \quad (7)$$

where,

$$\tilde{\mathbf{f}} \triangleq \mathbf{f} - (\mathbf{f}^T \Delta\mathbf{x}) \Delta\mathbf{x}. \quad (8)$$

Along the estimated normal vector  $\hat{\mathbf{e}}_f$ , force control is applied.

### 5 Adaptive hybrid visual servoing/force control

#### 5.1 Coordination of controllers

In the case that a robot has only one external sensor, a task for the robot is given on its sensor space,

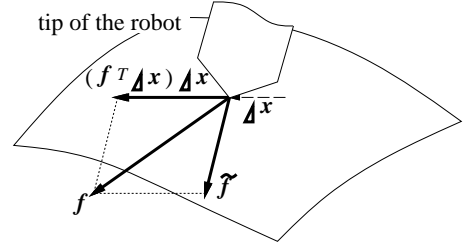


Figure 3: Sensed force is the sum of the frictional force and the normal force

and there is no need to coordinate external sensor based controllers. In [8], [9] and [10], the robot has only a force sensor. The force control and position control are both force sensor based control, therefore they need not consider the coordination between the controllers.

In the case that a robot has several external sensors, tasks for the robot are given in the sensor spaces. One must consider the coordination between the external sensor based controllers, because

- R1** the given tasks happen to be dependent on each other, because the tasks are given in different spaces independently, and
- R2** even if the tasks are well-considered beforehand so that the tasks can be independent of each other, they tend to suffer from noise and disturbances, and they become no more independent of each other.

In [11], Nelson et al. assume that all the parameters of the robot and the environment are known so that one can calculate the selection matrices which describes directions of force control and visual servoing control before the tasks are accomplished. Consequently, force control and visual servoing control can be applied independently, and they do not coordinate two controllers. In their case, however, the tasks for the visual servoing control and the force control must be well-considered beforehand so that they can be independent of each other, and the resultant controller is sensitive to disturbances.

When the parameters are unknown, one can estimate the image Jacobian matrix and the normal unit vector of the unknown constraint surface from the proposed estimators in the last two sections. However, because of the reasons **R1** and **R2**, the outputs of the visual servoing control are no more independent of those of the force control. In such a case, the manipulator may break the constraint surface and/or the manipulator itself, or it may not be able to keep contact with the surface. Therefore, to realize the hybrid visual servoing/force control one have to coordinate these controllers before applying them.

The force control task is prior to the visual servoing task, because the sampling rate of the force control is shorter than that of the visual servoing control, and

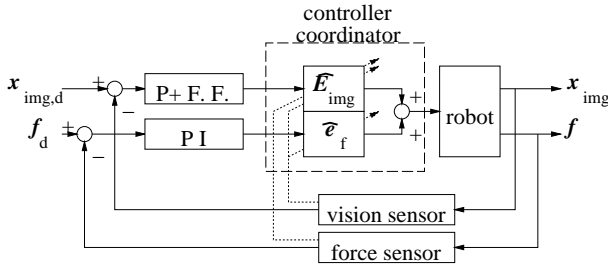


Figure 4: Adaptive hybrid visual servoing/force controller

because the result of the visual servoing control may break the constraint surface and/or the manipulator because it does not have force sensing, whereas the result of the force control may not. In this sense, one has to eliminate the force control direction  $\hat{e}_f$  from the image Jacobian matrix  $\hat{E}_{img}$ . The perpendicular matrix  $\hat{E}'_{img}$  becomes

$$\hat{e}'_{img,j} = \hat{e}_{img,j} - \hat{e}_{img,j} \hat{e}_f^T \hat{e}_f, \quad (9)$$

where  $\hat{e}'_{img,j}$ ,  $j = 1, \dots, m$  denote the row vectors of  $\hat{E}'_{img}$ . By utilizing eq.(9), the direction of the force control becomes perpendicular to those of the visual servoing control and therefore, one can coordinate the force control with the visual servoing control.

## 5.2 Adaptive hybrid visual servoing/force control

Suppose that the manipulator is controlled by the joint velocity controllers. In this paper, P+feed forward controller and PI controller are applied for visual servoing control and force control, respectively,

$$\dot{\theta} = J^{-1}(\mathbf{u}_f + \mathbf{u}_{img}), \quad (10)$$

where

$$\mathbf{u}_f = \hat{e}_f \left\{ K_{fp}(f_d - \hat{e}_f^T \mathbf{f}) + K_{fi} \int (f_d - \hat{e}_f^T \mathbf{f}) dt \right\}, \quad (11)$$

and

$$\mathbf{u}_{img} = \hat{E}'_{img} \{ \dot{\mathbf{x}}_{img,d} + \mathbf{K}_p(\mathbf{x}_{img,d} - \mathbf{x}_{img}) \}. \quad (12)$$

Vectors  $f_d$  and  $\mathbf{x}_{img,d}$  denote the desired force along the normal vector of the constraint surface and the desired image feature vector, respectively. Note that the robot Jacobian matrix  $J$  is known from the assumption **A1**. The adaptive hybrid visual servoing/force control is shown in figure 4.

## 6 Experiment

To show the effectiveness of the proposed estimators and hybrid controller, some experimental results are shown in this section.

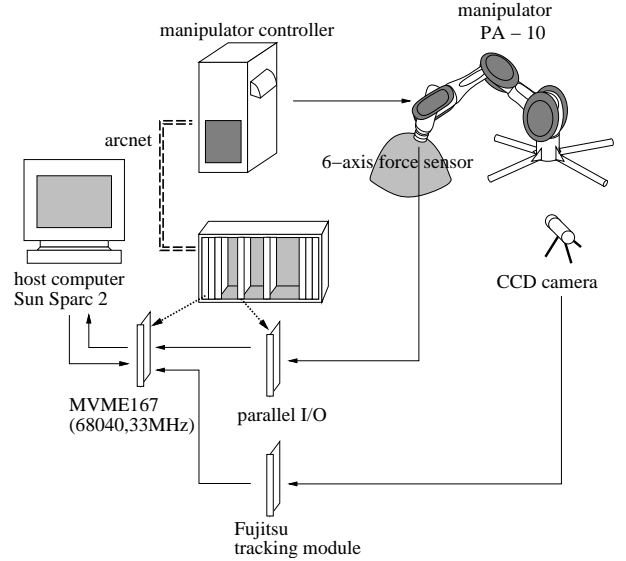


Figure 5: Experimental equipment

### 6.1 Experimental equipment

In figure 5, a camera-manipulator system used for experiments is shown. Video signal from a CCD camera is sent to a tracking unit equipped with a high-speed correlation processor by Fujitsu [14] (image size : 512[pixel]  $\times$  512[pixel]). We specify certain regions in the image (called templates) which we want the unit to track, before starting an experiment. During the experiments the unit feeds coordinates where the correlation measure (it uses a SAD measure, Sum of Absolute Difference) is the smallest with respect to the templates to the main control board MVME167 (CPU:68040, 33MHz, Motorola). Force signals obtained by a 6 axis force/torque sensor (BL autotech Ltd.) are also fed to the control board through a parallel I/O port. The control board calculates control signals for the manipulator by the proposed scheme and sends them to the manipulator controller via network(5Mbps). We use a 7 degree-of-freedom manipulator PA-10 (Mitsubishi Heavy Industry Co.) as a 3 degree-of-freedom manipulator, maintaining fixed desired orientation of the tip of the manipulator. Using this experimental equipment and writing programs using C language on VxWorks (Wind River), sampling rate of the visual servoing control and that of the force control are 33[ms] and 4[ms], respectively.

### 6.2 Experiments on a curved surface

An overview of the manipulator, the camera, and the constraint surface is shown in figure 6. The constraint surface is a curved one, whose shape is unknown. In this experiment, we use one camera. A desired image sequence given for the experiment is shown in figure 7. The desired image feature pattern is moving from point A to B in 5 [sec], B to C in 5[sec], and C to A in 5[sec] according to the trapezoidal velocity curves. The desired force along the normal of the

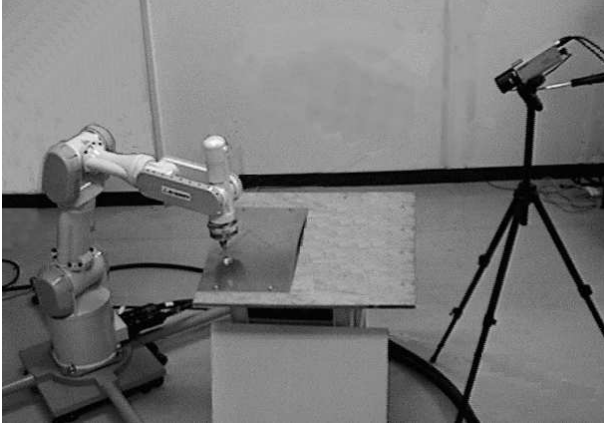


Figure 6: Overview of the manipulator, the camera, and the constraint surface

surface is 19.6[N]. The weighting matrix  $\mathbf{W}$  and the forgetting factor  $\rho$  are selected as  $0.01\mathbf{I}$  and 0.3, respectively, by trial and error. The initial value of the image Jacobian  $\hat{\mathbf{E}}_{img}$  is roughly estimated by simple movements along  $x$ ,  $y$ ,  $z$ -axis,

$$\hat{\mathbf{E}}_{img}(0) = \begin{bmatrix} -0.03 & 0.4 & -0.02 \\ 0.15 & 0.1 & -0.2 \end{bmatrix}.$$

As for gains,  $K_{fp} = 29.0$ ,  $K_{fi} = 0.075$ , and  $\mathbf{K}_p = \text{diag}[2.0 \ 2.0 \ 2.0]$ .

The experimental results, estimated normal vectors of the constraint surface, exerted normal force, a realized trajectory on the image plane, tracking errors on the image plane along  $x$  and  $y$  directions, are shown in figures 8–12. The estimates of the normal vectors look perpendicular to the curved constraint surface in figure 8. We can find that the proposed force control scheme can realize a good force response from figure 9. The force error becomes small when the speed of the manipulator becomes small. From figure 10, we can find that the proposed controller realizes a good response on the image plane, too. The tracking error on the image plane is less than 4 [pixels](figures 11 and 12).

We have also done an experiment without the coordination of force control and visual servoing control, and found that the resultant controller hit the constraint surface and almost break the manipulator. From this fact and these experimental results, we have shown the effectiveness of the proposed method.

## 7 Summary and Discussions

In this paper, an adaptive hybrid visual servoing/force controller has been proposed to accomplish the visual servoing task while it exerts the given force on an unknown constraint surface. The proposed controller only needs knowledge on the manipulator kinematics, and does not need any more. In this case of the

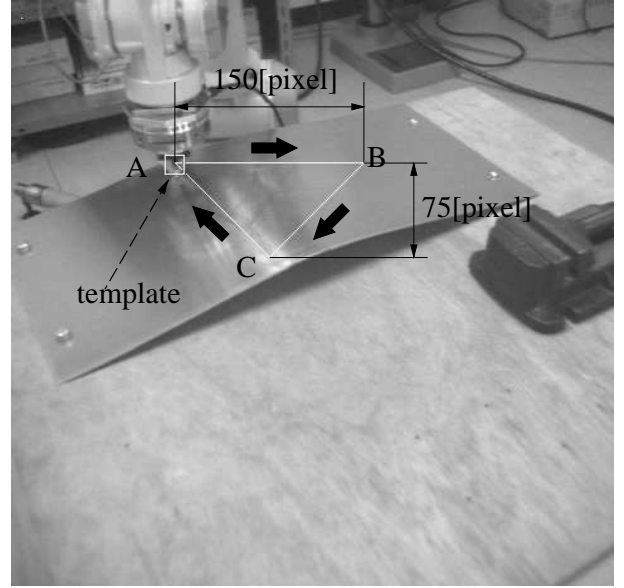


Figure 7: Desired image trajectory on the image plane

force and visual servoing controllers, we have made task priority that the force control is prior to the visual servoing control, and have coordinated these controllers. Some experimental results have demonstrated the effectiveness of the proposed scheme.

In [8], [9] and [10], the robot has only a force sensor. In these studies they apply force control along the given/estimated force direction, and apply position control, which is not an external sensor based control, along the perpendicular directions. Therefore, we can say that the force controller is not in the same control level as the position controller, but it obviously has exact priority to the position controller in these studies. In this sense, these controllers are *not* hybrid structure of several external sensor based controllers.

On the other hand, we have made a *hybrid structure* of two external sensor based controllers, the force controller and the visual servoing controller. The coordination of two controllers is derived from the task priority, depending on the given task and the situation. Note that the word “hybrid” means “hybrid structure of external sensor based controllers”, which is different from the traditional “hybrid control.”

This fact leads that it is important how to derive the task priority depending on the given task and the situation. As mentioned above, in the case of the visual servoing and the force control, the force control task is prior to the visual servoing task, because the sampling rate of the force control is shorter than that of the visual servoing control, and because the result of the visual servoing control may break the constraint surface and/or the manipulator since it does not have force sensing, whereas the result of the force control may not. But, in other cases, we have not found the

general principle to derive the task priority, yet.

We also have to mention to the degrees of freedom of the robot and the degrees of the given tasks. In the case that the number of degrees of freedom of the robot is sufficient to realize the given tasks, one do not have to care about the priority of the tasks, but otherwise one have to. When the robot is achieving a sequence of tasks, one have to consider how many degrees of freedom are needed to achieve the tasks and how to derive the task priority. For example, when the robot has two cameras, one have to coordinate controllers more severely, because the visual servoing task will be conflict with the force control task.

To coordinate several external sensor based controllers, they have to have a common coordinate frame where two schemes are coordinated. It is also the case to coordinate the visual servoing control with the force control. This is a reason why we have made the image features on the tip of the manipulator, and why we have made the assumption **A1**. In this case, the manipulator base frame becomes the common frame between two control schemes. In a case that other sensors are applied, one have to consider the common frame to coordinate.

## References

- [1] P. I. Corke. Visual control of robot manipulators – a review. In *Visual Servoing*, pages 1–31. World Scientific, 1993.
- [2] W. Jang and Z. Bien. Feature-based visual servoing of an eye-in-hand robot with improved tracking performance. In *Proc. of IEEE Int. Conf. on Robotics and Automation*, pages 2254–2260, 1991.
- [3] N. Maru, H. Kase, et al. Manipulator control by visual servoing with the stereo vision. In *Proc. of the 1993 IEEE/RSJ Int. Conf. on Intelligent Robots and Systems*, pages 1865–1870, 1993.
- [4] K. Hashimoto, T. Kimoto, T. Ebine, and H. Kimura. Manipulator control with image-based visual servo. In *Proc. of IEEE Int. Conf. on Robotics and Automation*, pages 2267–2272, 1991.
- [5] L. E. Weiss, A. C. Sanderson, and C. P. Neuman. Dynamic sensor-based control of robots with visual feedback. *IEEE J. of Robotics and Automation*, RA-3(5):404–417, 1987.
- [6] J. T. Feddema and C. S. G. Lee. Adaptive image feature prediction and control for visual tracking with a hand-eye coordinated camera. *IEEE Trans. on System, Man, and Cybernetics*, 20(5):1172–1183, 1990.
- [7] B. Nelson, N. P. Papanikolopoulos, and P. K. Khosla. Visual servoing for robotic assembly. In *Visual Servoing*, pages 139–164. World Scientific, 1993.
- [8] M. H. Raibert and J. J. Craig. Hybrid position/force control of manipulators. *ASME Journal of Dynamic Systems, Measurement, and Control*, 103(2):126–133, 1981.
- [9] T. Yoshikawa and A. Sudo. Dynamic hybrid position/force control of robot on-line estimation of unknown *IEEE Trans. on Robotics and Automation*, 9(2):220–225, 1993.
- [10] A. Fedele, A. Fioretti, C. Manes, and G. Ulivi. On-line processing of position and force measures for contour identification and robot control. In *Proc. of IEEE Int. Conf. on Robotics and Automation*, pages 369–374, 1993.
- [11] B. J. Nelson, J. D. Morrow, and P. K. Khosla. Improved force control through visual servoing. In *Proc. of the American Control Conference*, 1995.
- [12] K. Hosoda and M. Asada. Versatile visual servoing without knowledge of true jacobian. In *Proc. of the 1994 IEEE/RSJ Int. Conf. on Intelligent Robots and Systems*, pages 186–193, 1994.
- [13] P. Eykhoff. *System Identification*, chapter 7. John Wiley & Sons Ltd., 1974.
- [14] M. Inaba, T. Kamata, and H. Inoue. Rope handling by mobile hand-eye robots. In *Proc. of Int. Conf. on Advanced Robotics*, pages 121–126, 1993.

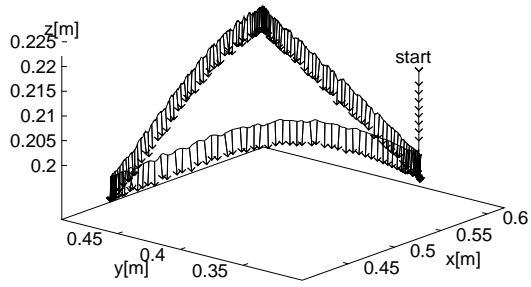


Figure 8: Experimental result 1:estimated normal vectors of the constraint surface

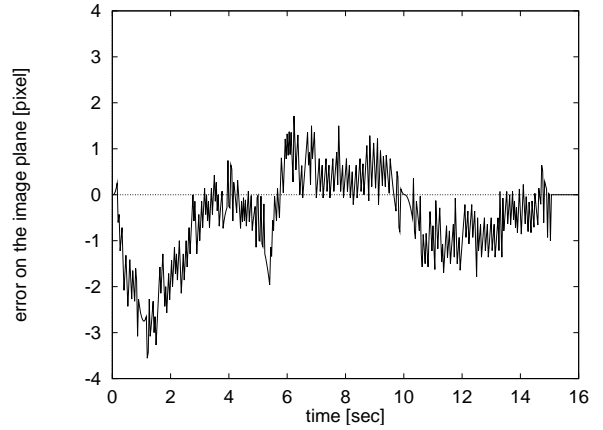


Figure 11: Experimental result 4:tracking error on the image plane(along  $x$ -axis)

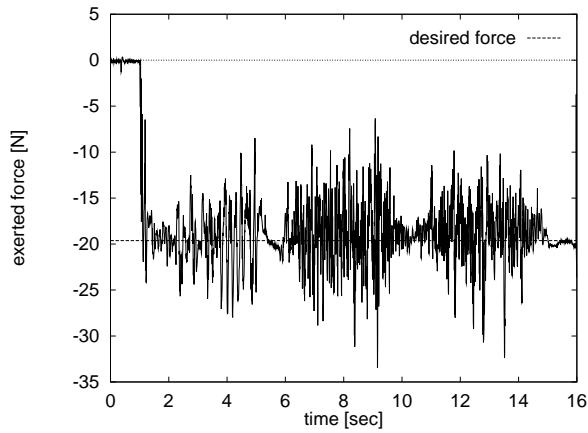


Figure 9: Experimental result 2:exerted normal force

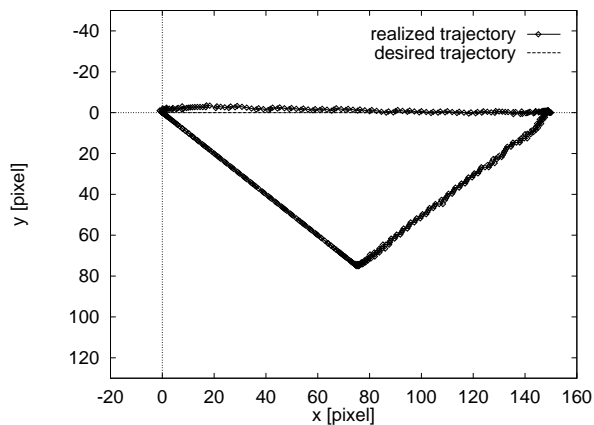


Figure 10: Experimental result 3:trajectory on the image plane

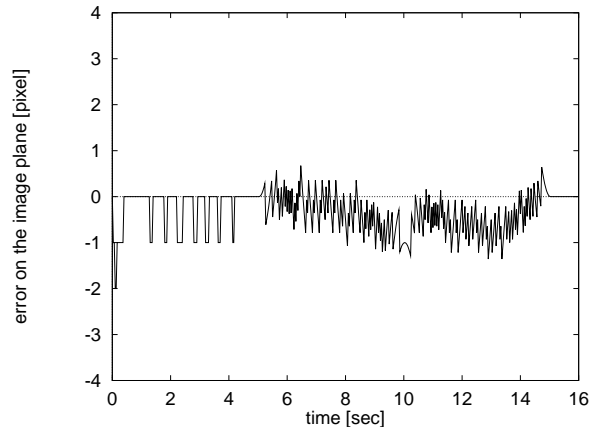


Figure 12: Experimental result 5:tracking error on the image plane(along  $y$ -axis)